Journal of Thermal Engineering, Vol. 4, No. 3, pp. 1896-1911, April, 2018
Yildiz Technical University Press, Istanbul, Turkey

AEROTHERMAL OPTIMIZATION OF SQUEALER GEOMETRY IN AXIAL FLOW TURBINES USING GENETIC ALGORITHM

K. Deveci[1], H. Maral[2], C. B. Şenel[2], E. Alpman[3], L. Kavurmacıoğlu[2], C. Camcı[4]

ABSTRACT

In turbomachines, a tip gap is required in order to allow the relative motion of the blade and to prevent the blade tip surface from rubbing. This gap which lay out between the blade tip surface and the casing, results in fluid leakage due to the pressure difference between the pressure side and the suction side of the blade. The tip leakage flow causes almost one third of the aerodynamic loss and unsteady thermal loads over the blade tip. Previous experimental and numerical studies revealed that the squealer blade tip arrangements are one of the effective solutions in increasing the aerothermal performance of the axial flow turbines. In this paper the tip leakage flow is examined and optimized with the squealer geometry as a means to control those losses related with the tip clearance. The squealer height and width have been selected as design parameters and the corresponding computational domain was obtained parametrically. Numerical experiments with such parametrically generated multizone structured grid topologies paved the way for the aerothermal optimization of the high pressure turbine blade tip region. Flow within the linear cascade model has been numerically simulated by solving Reynolds Averaged Navier-Stokes (RANS) equations in order to produce a database. For the numerical validation a well-known test case, Durham cascade is investigated in end wall profiling studies has been used. Sixteen different squealer tip geometries have been modeled parametrically and their performance have been compared in terms of both aerodynamic loss and convective heat transfer coefficient at blade tip. Also, these two values have been introduced as objective functions in the optimization studies. A state of the art multi-objective optimization algorithm, NSGA-II, coupled with an Artificial Neural Network is used to obtain the optimized squealer blade tip geometries for reduced aerodynamic loss and minimum heat transfer coefficient. Optimization results are verified using CFD.

Keywords: *Multi-objective Optimization, Squealer, Tip Leakage Flow*

INTRODUCTION

The spacing between the blade tip of an axial flow turbine and the casing is significant source of inefficiency. The tip leakage flow, induced by the pressure difference between the pressure and suction sides of the blade tip, is responsible for the one third of the aerodynamic losses at a turbine stage [1, 2]. The pressure driven flow rolls into leakage vortex downstream of the suction side and interacts with the main passage flow. Highly complex flow structures near the blade suction side results with decrease in aerothermal performance of the axial turbine. The tip leakage flow also does not contribute to the work extraction from the fluid since the leakage flow is not turned as the passage flow [3, 4, 5]. Instead, the leakage flow reduces work generation due to the reduction in the main flow rate through the blade passage [2,6]. In addition to the aerodynamic perspective, the blade tip surface is exposed to hot gas stream which cause higher thermal loads on the blade tip [5,7].

This leakage flow passing through tip gap without experiencing any expansion or cooling, can create important turbine durability problems at the blade tip. There have been many studies in the literature that investigates the tip leakage flow both numerically and experimentally in order to clarify the flow physics and to reduce adverse effects of it. One of the most widely used methods to reduce tip leakage effects is using of squealer geometries. Moore and Tilton [8] investigated the leakage flow experimentally in a linear cascade turbine arrangement and developed an analytical

This paper was recommended for publication in revised form by Regional Editor Tolga Taner
[1]Department of Energy Science & Technology, Istanbul Technical University, Istanbul, TURKEY
[2]Department of Mechanical Engineering, Istanbul Technical University, Istanbul, TURKEY
[3]Department of Mechanical Engineering, Marmara University, Istanbul, TURKEY
[4]Department of Aerospace Engineering, Pennslyvania State University, PA, USA
**E-mail address: emre.alpman@marmara.edu.tr*
Manuscript Received 28 October 2016, Accepted 20 March 2017

model considering the potential flow theory. Bindon [9] experimentally investigated the tip leakage flow in a linear turbine cascade for a sharp corner and obtained that internal gap loss corresponded to the 39% of the total loss while mixing loss near the suction side formed the 48%. Study by Yaras and Sjolander states that kinetic energy carried by the normal velocity component of the leakage flow was lost [10]. Tallman and Lakshminarayana [11] carried out a numerical investigation on the effect of the tip gap height on the leakage flow. Studies indicate that relative motion between the blade tip and the casing increases the leakage flow rate in compressors while it decreases in turbines [12, 13].

There have been various studies in order to improve the aerothermal performance of the turbomachine by weakening the tip leakage flow and its' interactions with the passage flow. Passive control methods such as cavity squealer, partial squealer and winglet designs are widely investigated to mitigate the tip leakage related loss. Heyes et al. [3] observed a significant aerodynamic reduction in losses with squealer designs. Ameri et al. [14] numerically investigated the effect of squealer designs on heat transfer together with efficiency and stated that use of squealer rims reduces leakage flow rate while increases the heat transfer at blade tip. Krishnababu et al. [4] numerically investigated the different squealer geometries and specified that with an increase in tip clearance, the leakage mass flow and the heat transfer to the tip is increased. Azad et al. [5] examined 6 different types of squealer geometries in a linear turbine cascade experimentally and results revealed that the suction side squealer offered better aerothermal performance compared to the cavity squealer and pressure side squealer. Camci et al. [15] carried out an experimental study on the aerodynamic performance of partial squealer rims in a low speed rotating axial flow turbine facility and obtained that suction side squealer had better performance than the cavity squealer. Kavurmacioglu et al. [16] performed a numerical study on the aerodynamic performance of the different blade tip designs and the numerical predictions revealed that partial squealer designs reduced the aerodynamic loss compared to the flat tip. A numerical investigation by Krishnababu et al. [4] showed that cavity squealer design reduced both the aerodynamic loss and the heat transfer to the blade tip. An experimental study on the flow structure over a cavity squealer design by Lee and Kim [17] showed that cavity squealer reduced the aerodynamic loss with respect to the flat tip in a linear cascade test rig. Zhou and Hodson [18] used experimental and numerical methods to investigate the both aerodynamic and thermal performance of the cavity squealers for different squealer height and width and showed that both thickness and height of the squealer play an important role to improve the performance of the turbomachine. Schabowski and Hodson [2] investigated the effects of the squealer and winglet designs on the tip leakage flow structure and obtained that winglet designs can be used in order to reduce the driving pressure and to weaken the tip leakage vortex.

In recent studies, contoured blade tip designs have been suggested in order to diminish the leakage flow rate and reduce the thermal loads on the blade tip surface. De Maesschalck et al. [19] investigated the aerothermal performance of two fully carved blade tip designs. De Maesschalck et al. [20] geometrically optimized the blade tip sections in order to deal with tip leakage losses by tip carving and stated that many heterogeneous tip geometries exist that can offer increase aerothermal performance.

In this study, a state of the art multi-objective optimization algorithm (NSGA-II) coupled with artificial neural network (ANN) is used to obtain optimized squealer geometries for subsonic flows. The objective functions are selected as the heat transfer coefficient and the aerodynamic loss. Optimization parameters are determined as the squealer width and the squealer height. To the best of our knowledge, this is the first work that shows an artificial intelligence based multi-objective optimization of squealer geometry in the literature. There have been many studies that investigate the effect of the squealer and height, however there is no studies in order to obtain optimum squealer dimensions considering the aerodynamic and thermal effects using a multi-objective optimization method.

The remainder of this paper is organized as follows. Section-II describes the proposed methodology for tip leakage flow optimization. In Section-III, initial database, optimized geometries, and their objective function values are given and CFD results are discussed. In Section-IV we give a conclusion.

METHODOLOGY

The present study develops an artificial intelligence based multi-objective optimization strategy to produce a set of optimized solutions for the tip leakage problem considering both aerodynamic losses and thermal loads on the blade tip surface. Since experimental measurements are expensive, difficult and highly challenging for tip leakage

flows in turbomachinery, the tip leakage flow is numerically simulated by solving 3D incompressible and steady Reynolds Averaged Navier Stokes (RANS) equations. For geometrical optimization of the squealer rim, NSGA-II algorithm which was developed by Deb et al. [21], coupled with an ANN is used. The results obtained from the NSGA-II & ANN system are verified using CFD.

NSGA-II

Multi-objective evolutionary algorithms search for a set of optimum solutions (Pareto set) instead of a single optimum solution searched by single objective optimization methods [21]. In multi-objective evolutionary optimization literature, an individual is said to *dominate* another individual, if and only if the objectives of the former are better than the objectives of the latter. The solutions which are not dominated by other solutions form the Pareto optimum solution set for the problem studied. NSGA-II is one of the most efficient state of the art population based evolutionary algorithms designed for multi-objective optimization problems [22-24]. It simulates the Darwinian evolution principle where the population of individuals are evolved and adapted with reproduction mechanisms such as crossover and mutation, and finds an appropriate set of solutions for the problem. NSGA-II uses non-dominated sorting technique together with a crowding distance approach to rank and select individuals and produce population fronts [21]. In this paper, an in-house developed real parameter NSGA-II optimization code originally shared by Aravind Seshadri [25] is modified and used.

Artificial Neural Networks (ANN)

For this study, the objective values of the individuals are needed to be calculated accurately and efficiently at each function evaluations. Since there is no simple aerodynamic model to predict the aerodynamic loss and the amount of heat transfer at the tip, CFD tools may be resorted to compute these quantities. 3D analysis of complex tip leakage flow with CFD tools is highly time consuming, therefore using a metamodel to perform the performance predictions plays a significant role in reducing the required time for optimization. For this purpose, ANN is used as a mathematical interpolator to find accurate estimations of the objective functions.

Preparing ANN before using it as an objective function evaluator requires 3 main steps:

1. Preparing a set of initial database
2. Building neural networks (includes training, validation, and testing)
3. Selecting the best network in terms of performance

In general, the best neural network is selected according to its' performance which is evaluated by the test data. Here, a number of networks are first created and then each network is trained and tested according to the accuracy of their predictions. One method to check the accuracy of predictions is to calculate the *mean square error* which is expressed as:

$$\mathrm{MSE} = \frac{1}{\mathrm{n}} \sum_{\mathrm{i}=1}^{\mathrm{n}} (\widehat{\mathrm{Y}}_{\mathrm{i}} - \mathrm{Y}_{\mathrm{i}})^2 \tag{1}$$

In equation (1) $\hat{Y}_i$ represents vector of test predictions and Y_i represents the vector of actual data. Numerical experience showed that this expression is not enough to select the best network when the number of solutions in database is limited. Selected ANNs based on this performance formulation were not able to accurately predict its' training data. For this reason, the definition of mean square error for ANN performance is revised and the accuracy of both training and testing data is determined together:

$$\mathrm{MSE}_{\mathrm{New}} = \mathrm{a}\left[\frac{1}{\mathrm{n}} \sum_{\mathrm{i}=1}^{\mathrm{n}} (\widehat{\mathrm{Y}}_{\mathrm{T}} - \mathrm{Y}_{\mathrm{T}})^2\right] + \mathrm{b}\left[\frac{1}{\mathrm{n}} \sum_{\mathrm{i}=1}^{\mathrm{n}} (\widehat{\mathrm{Y}}_{\mathrm{R}} - \mathrm{Y}_{\mathrm{R}})^2\right] \tag{2}$$

Here $\hat{Y}_T$ represents vector of predictions for testing data, Y_T represents the actual vector of testing data, $\hat{Y}_R$ represents the vector of training data predictions, and Y_R represents the actual vector of training data. The terms a and b are the weights of the error terms and they depend on the set of solutions in database.

As a function fitting tool, feedforward neural network (FFNN) architecture is used. Some successfully implemented FFNN based optimization studies in different fields can be found in [27-33]. In our case, FFNNs are trained with Levenberg - Marquardt algorithm by using MATLAB Neural Network Toolbox. During training, both inputs and outputs are normalized between [-1,1]. The best network is selected with the performance function given by Eq. 2.

Defining Design Variables and Objective Functions

The squealer height (s) and the squealer width (w) correspond to the design variables and defined in Figure 1. The flow structure within the tip gap is an important source of inefficiency in terms of aerodynamic loss and heat transfer to the blade tip. For this reason, the objectives of the problem are determined as the aerodynamic loss coefficient and the average heat transfer coefficient which are aimed to be minimized. For the present study, aerodynamic loss is quantified using total pressure loss coefficient and amount of heat transfer is quantified using the average heat transfer coefficient at the tip region. The total pressure coefficient (C_{P0}) is defined as the difference in

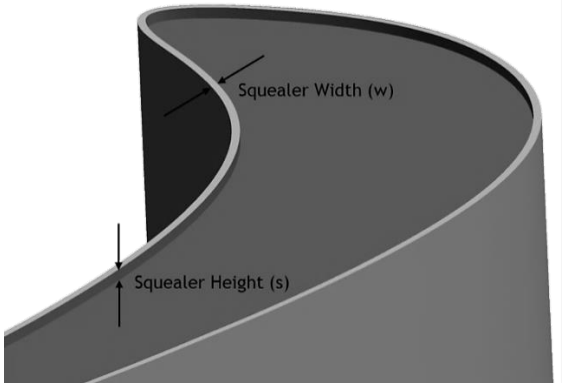

Figure 1. Design variables of the problem.

total pressure between the inlet and exit plane of the cascade located at $0.05C_x$ distance downstream of the trailing edge. C_{P0} is given in Eq. 3 where P_{01} is the mass flow averaged total pressure at inlet and U_m is the reference velocity obtained from AFTRF test rig.

$$C_{p0} = \frac{P_0 - P_{01}}{0.5\rho U_m^2} \tag{3}$$

The total pressure loss coefficient ΔC_{p0} is calculated at the exit plane of the linear cascade as in Eq. 4.

$$\Delta C_{p0} = \frac{\iint \rho u C_{p0} dydz}{\iint \rho u dydz} \tag{4}$$

The local heat transfer coefficient (h), on the other hand, is defined as the ratio of wall heat flux (q_w) to temperature difference between wall temperature (T_w) and mass averaged total temperature at inlet ($T_{0,in}$). Area average heat transfer coefficient $\bar{h}$ is then calculated on blade tip and squealer upper surfaces.

$$\bar{h} = \frac{q_w}{T_w - T_{0,in}} \tag{5}$$

The mass flow averaged total temperature at the inlet of the domain has been used in order to calculate the heat transfer coefficient as suggested by Ameri [14] and Krishnababu [4].

Proposed NSGA-II & ANN Optimizer

In this study, feedforward neural networks with one hidden layer are used. To find a good network for fitting purposes, the number of neurons inside the hidden layer is changed between 2 to 10, and all hidden layer constructions are trained 10 times. In other words, 90 samples of ANN are created and trained. After ANN trainings are completed, the best network is chosen based on Eq. 2 among the 90 networks studied. The structural representation of the selected neural network can be found in Figure 2. It consists of 2 neurons in the input layer, 5 neurons in the 1 hidden layer, and 2 neurons in the output layer.

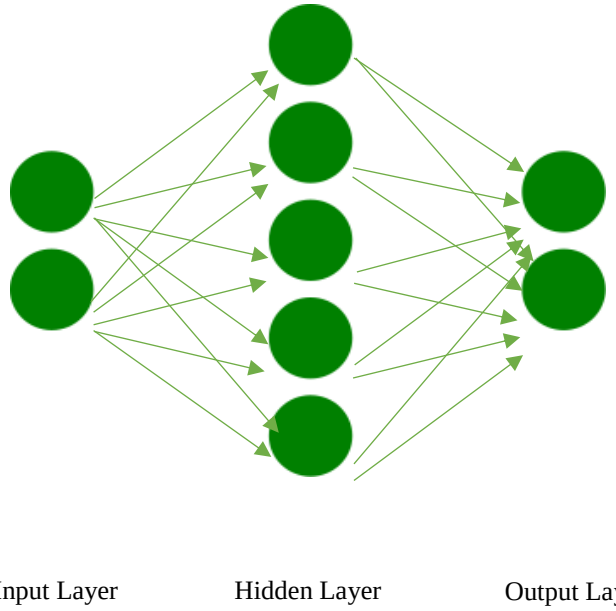

Figure 2. Structural representation of the selected neural network

Next, the selected network is implemented in NSGA-II code as an objective function evaluator. In every generation, objective values of each individual are calculated from the predictions of the embedded neural network. The utilized NSGA-II code in this research uses Simulated Binary Crossover (SBX) and polynomial mutation. The parameters of NSGA-II & ANN coupled system are given in Table 1 and Table 2.

Table 1. Parameters on NSGA-II

Population Size	100
Generation number	200
Mutation Rate	0.2
Crossover Rate	0.8
Mutation Index	20
Crossover Index	20
Tournament Size	5

The suggested selection mechanism for NSGA-2 is binary tournament selection [21]. For research purposes, we used tournament size as 5 in this research.

Table 2. Parameters of ANN

Normalization Interval	[-1,1]
a	0.3
b	0.7
Number of hidden layers	1

Refer to Eq. 2 for a and b

III. RESULTS & DISCUSSION

Initial database which contains 16 solutions, is created using 4 level full factorial approach. The selected values of squealer height, squealer width, and their objective function values obtained by using CFD tools are given in Table 3. Squealer heights in Table 3 are given non-dimensionally in terms of tip gap height (*t*).

Typically, neural networks are trained, validated, and tested with 70%, 15%, and 15% of the database solutions respectively. Since the database is very limited in this research, validation set is omitted and 15 solutions in the database are used for training and the remaining solution was used for testing. The selected training and test data are shown in Figure 3 using solid circle and diamond symbols, respectively. As it can be seen from Table 3, the aerodynamic losses and heat transfer coefficients are better for higher squealer heights.

Table 3. Initial database

		w02	**w04**	**w06**	**w08**
s16	ΔC_{P0}	-0.132	-0.132	-0.132	-0.13
	$\bar{h}$	320.2	364.3	329.7	337.7
s26	ΔC_{P0}	-0.125	-0.128	-0.120	-0.124
	$\bar{h}$	283.9	329.7	276.8	280.6
s36	ΔC_{P0}	-0.12	-0.113	-0.119	-0.121
	$\bar{h}$	255.2	272.1	232.1	250.3
s46	ΔC_{P0}	-0.114	-0.109	-0.116	-0.113
	$\bar{h}$	203.2	208.5	178.6	198.8

In order to maintain the good performance of the neural network, the test data is not selected from the 0.82 mm height level. This height level also includes the best aerodynamic and thermal performances. Choosing the test data from lower levels (0.205mm) could also mislead the post-processing study, so the test data is selected from 0.615mm height level as shown in Figure 3. Since in the literature MSE values are calculated from test data, the weight of testing error is expected to be higher than the weight of training error. Therefore, during MSE calculations, *a* and *b* values are selected as 0.3 and 0.7, respectively.

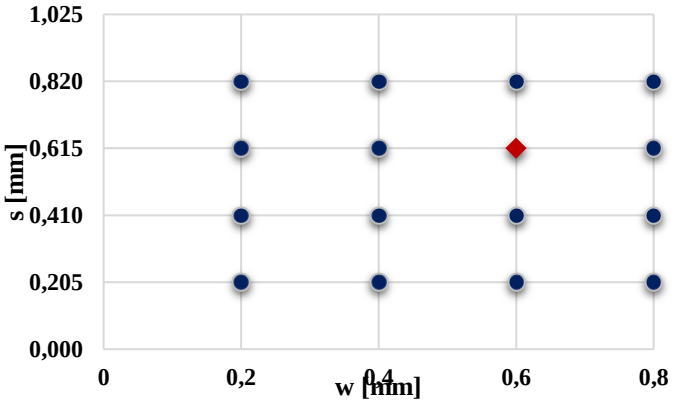

Figure 3. Solution parameters of database.

Optimized Geometries

The optimization studies are performed with 100 individuals and 200 generations. The fitness values of the individuals at different generations and the final Pareto front is displayed in Figure 4. From this figure one can easily see the convergence of the individuals towards the final Pareto front beyond which no more improvement is physically possible.

The final Pareto front provides a trade-off between objective functions. Since all the solutions on the Pareto front is non-dominated (one cannot say that an individual is better than the other) they can all be selected as an optimum solution to the problem.

Here we note that the obtained Pareto set is a non-dominated set based on the created model. It cannot guarantee that all solutions within this set will give the exact results when they are tested. For our case, three solutions which provides minimum aerodynamic loss, minimum heat transfer and an average aerothermal performance are selected from the Pareto front. These three selected points are shown in Figure 5 with red triangles on the final Pareto front.

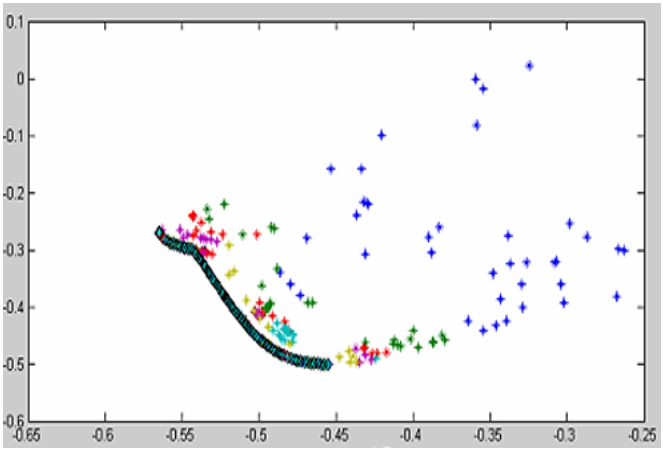

Figure 4. Final Pareto front (normalized).

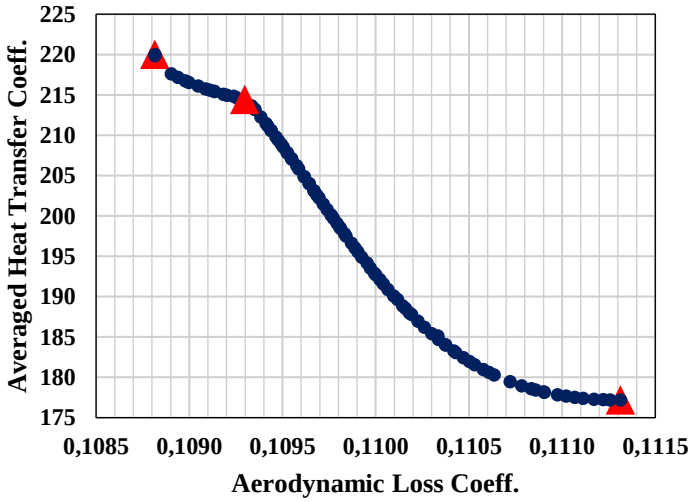

Figure 5. Final Pareto front (denormalized).

CFD Results of Optimum Geometries

The Computational Fluid Dynamics (CFD) method becomes an important tool to analyze the complex flow structures within the tip gap. Considering the number of the cases for CFD computations, solid model and grid have been parametrically generated in order to reduce production time. 16 squealer tip geometries are modeled in a

parametric way related to design parameters for 4 different rim heights (*s*) and 4 different rim widths (*w*). For modeling computational domain, a 3D modelling module, ANSYS SpaceClaim is used. The domain is divided into multi-blocks for the high quality mesh generation in a simple manner as shown in Figure 6.

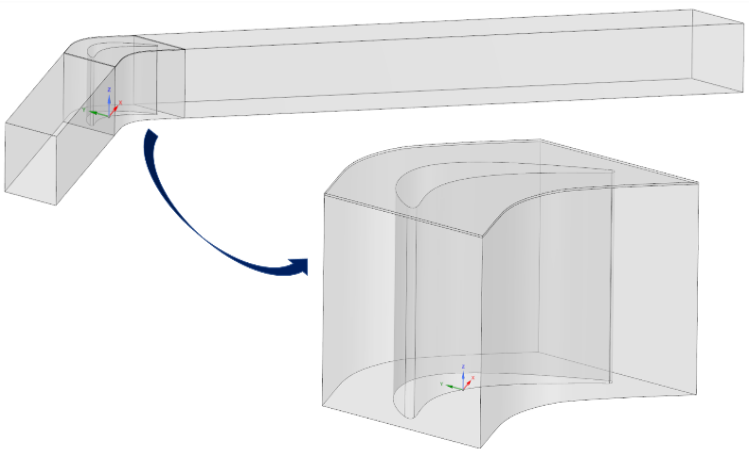

Figure 6. Multi-blocked computational domain.

The inlet domain has the length of $2.0C_x$ and the outlet domain $6.0C_x$. The rotor domain has been divided into two main parts: blade domain and tip domain for controlled mesh. In order to decrease the solution time while maintaining sufficient accuracy for the solutions, fully hexagonal mesh is used. The y+ value is kept around 1 using boundary layer mesh topology all around the turbine blade.

Figure 7 and Figure 8 show the hexagonal mesh around the blade and the squealer rim. The axial turbine blade geometry shown in these figures belongs to the Pennsylvania State University Axial Flow Turbine Research Facility (AFTRF). Solid model of the axial turbine is modeled by extrusion of AFTRF tip profile in spanwise direction. Some design features of the turbine blade are given in Table 4.

Table 4. Blade specifications.

Specification	Value
Blade Height [mm]	123
Axial Chord [mm]	85.04
Inlet Flow Angle [°]	71.3
Pitch [mm]	99.274

Steady, 3D Reynolds Averaged Navier-Stokes (RANS) equations are solved using a finite volume discretization. The CFD analysis is performed using the commercial code, ANSYS CFX. For boundary conditions, mass flow at inlet and static pressure at outlet are applied for all cases. Turbulence intensity and length scale at inlet are defined as 0.5% and 0.123 m respectively. For thermal boundary conditions, inlet and wall temperatures are set as 50°C and 25°C respectively. Maximum Mach number in the computational domain is less than 0.3, hence compressibility effects are assumed to be negligible.

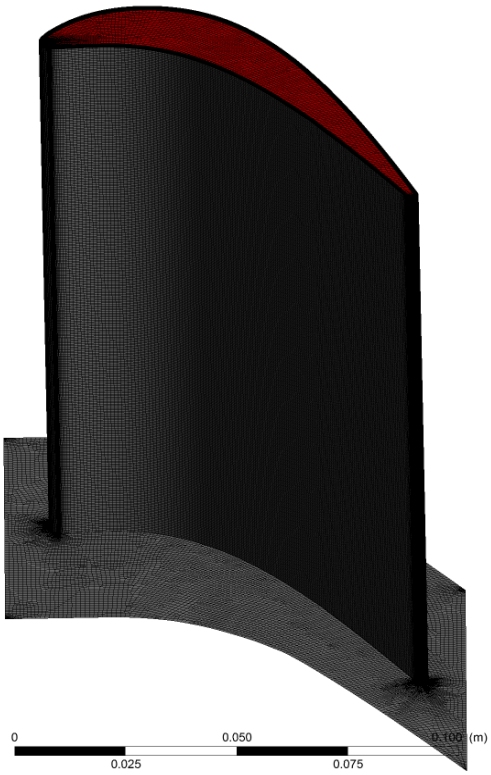

Figure 7. Fully hexagonal mesh around the blade and at hub.

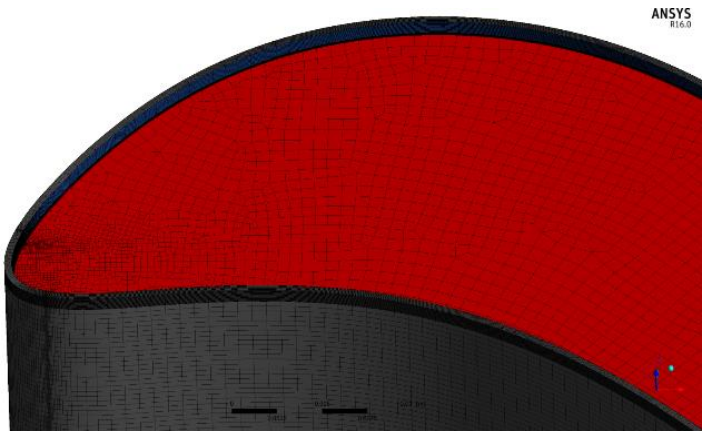

Figure 8. Mesh around the blade surface and squealer rim.

Shear Stress Transport (SST) model is used in the computations. In order to use the SST model, y^+ values should be less than 2 in the vicinity of the solid walls. This requirement is satisfied for all cases studied. In order to resolve the highly complex flow structures accurately and to reduce the aspect ratio of the cells in the vicinity of the wall, a large number of elements are used in the solutions, which resulted in a total number of cells of approximately 17 million.

For validation purposes, selected 3 results from the Pareto front obtained by NSGA-II & ANN coupled optimizer are reevaluated with CFD. Total pressure loss coefficient and average heat transfer coefficient predictions

for these three points obtained by using ANN and CFD are summarized in Table 5 along with the percent difference between the former and the latter. Despite the limited number of data used to train the networks, ANN predictions are generally in good agreement with CFD predictions except for the heat transfer coefficient for 0.297 mm squealer thickness.

Table 5. Comparison of the ANN and CFD predictions

w [mm]	**0.244**	**0.297**	**0.527**
ΔC_{p0-ANN}	-0.11	-0.11	-0.11
ΔC_{p0-CFD}	-0.11	-0.11	-0.12
Difference (%)	-3.18	-3.46	-4.91
$\bar{h}_{ANN}$ [W/m^{2}K]	202.22	219.99	177.19
$\bar{h}_{CFD}$ [W/m^{2}K]	194.79	184.25	183.31
Difference (%)	3.82	19.4	-3.34

Squealer heights are 0.82 mm in all selected geometries.

The predicted fitness values of these three solutions along with the initial database points are displayed in Figure 9. It is clear that the initial database could not dominate two of the three solutions selected and the best aerodynamic and the best thermal performances could not be further improved. Keeping the optimum aerodynamic and thermal solutions as pivot solutions, the aerothermal performance of other 14 solutions are successfully optimized.

Using the initial database and the selected 3 solutions from the final Pareto front, an initial and a final theoretical Pareto fronts are drawn in Figure 9 and Figure 10 by fitting second order polynomials to those three points. After optimization, the theoretical Pareto front is clearly improved. This means that any solutions taken from the final Pareto front dominates the previous solutions together with any possible solutions between two fronts which are not explored yet in this study. It is important to note that these are theoretically drawn Pareto fronts and their resolution is low. In other words, they are obtained with using only 3 points, the real Pareto front would be much more complicated than a second order polynomial. Compared to the blade with a flat tip, the best aerothermal solution offers 17.6% reduction in aerodynamic losses and 55.6% reduction in convective heat transfer coefficient.

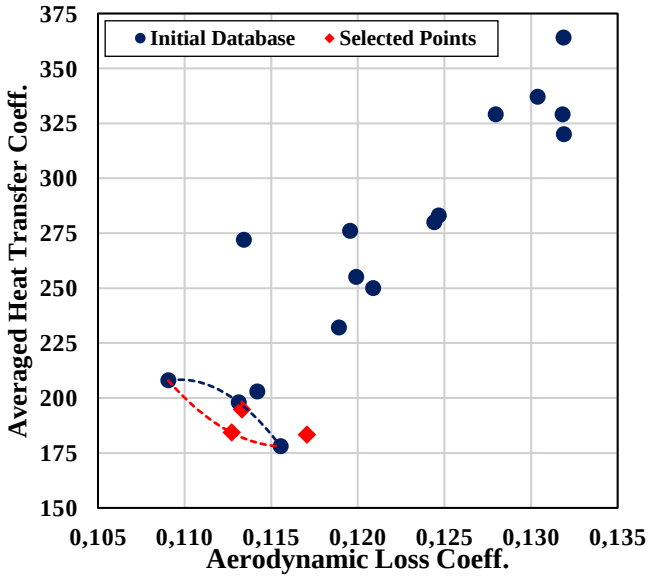

Figure 9. Comparison of optimized geometries with database.

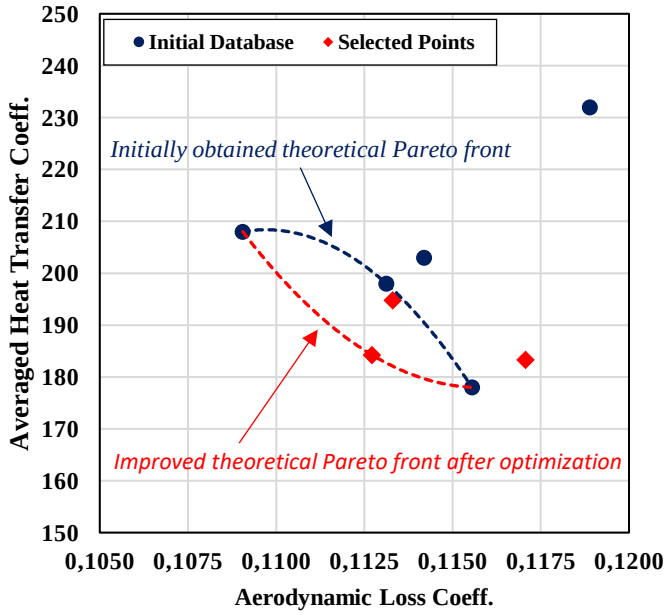

Figure 10. Advancement of theoretical Pareto front after optimization.

In order to validate the CFD method used for optimization purposes, pressure coefficient predictions obtained for the Durham cascade [26] are compared with the experimental data from reference [26] in Figure 11. Except the trailing edge region of the pressure side predictions are in good agreement with measurements.

The aerodynamic loss and the heat transfer coefficients of the flat tip geometry are calculated as -0.13682 and 415.4 W/m^{2}K respectively. Maximum value of y^+ is 0.34 around the blade profile at the 0.99h and therefore, y+ condition was satisfied for the optimum squealer geometry.

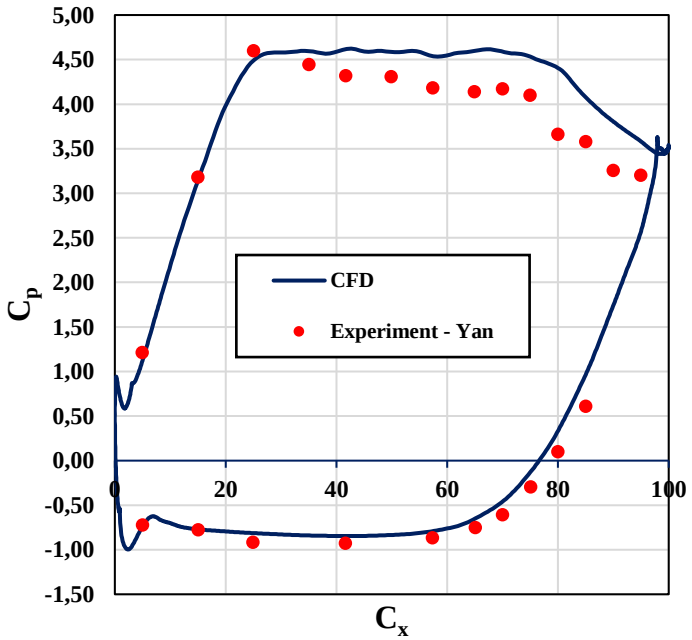

(a)

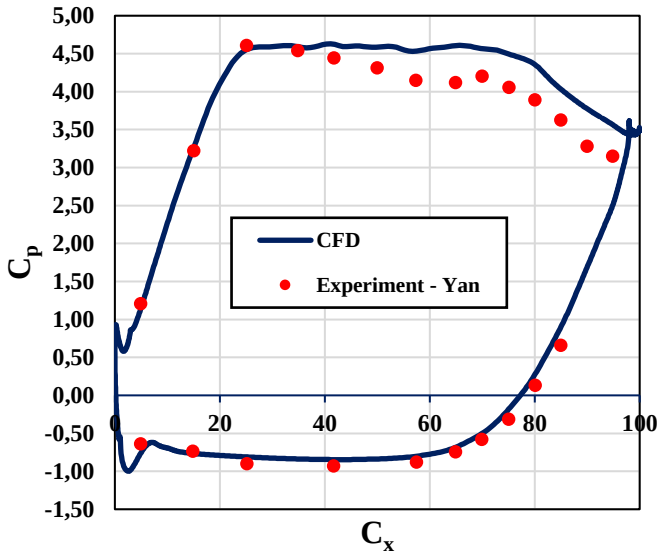

(b)

Figure 12. Comparison of C_p predictions with measurements (a) at 0.50h (b) 0.25h [26].

Aerothermal Investigation on Optimum Squealer Geometry

In this section, the aerothermal performance of the selected geometry is compared to that of the flat tip geometry, which represents the tip geometry without any tip treatment. According to the optimization results, the squealer geometry with a width of 0.297mm and height of 0.82 mm (will be denoted as SQw0297s46) gave the best aerothermal performance. The solid model of this optimum geometry is shown in Figure 12.

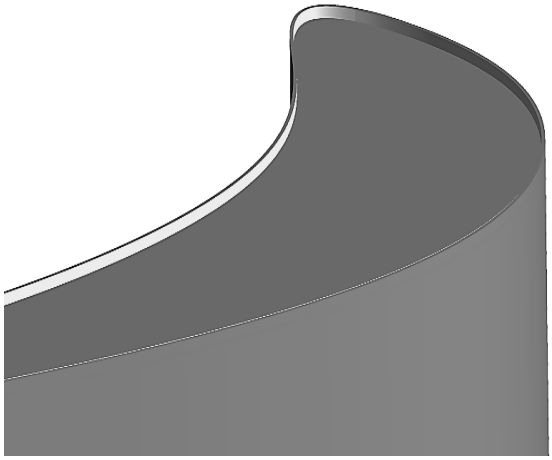

Figure 12. Optimum squealer geometry: SQw0297s46.

In Figure 13 total pressure coefficient distribution at exit plane is given in dimensionless form for flat tip and SQw0297s46 geometries. The total pressure distribution downstream of the trailing edge provides significant information about the loss mechanisms. Lower the total pressure means higher aerodynamic loss. It is evident from Figure 13 that SQw0297s46 has quite effective in reducing aerodynamic loss, occupation area by the leakage vortex and the corresponding momentum deficit compared to the flat tip.

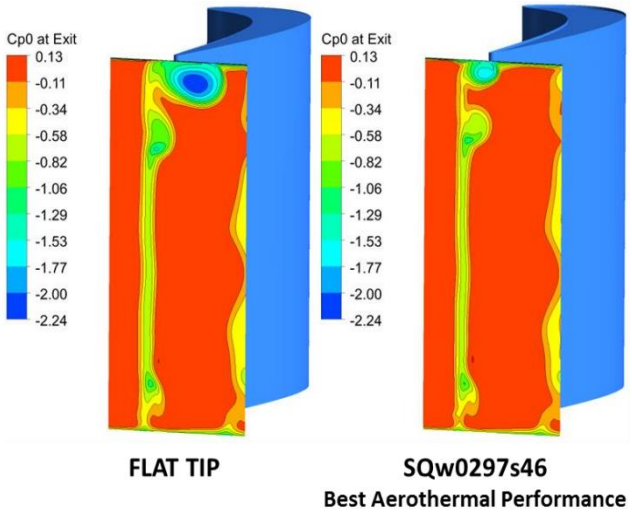

Figure 13. Total pressure coefficient at exit plane.

Figure 14 demonstrates the distribution of heat transfer coefficient at blade tip. Heat transfer coefficient decreases from pressure side to suction side due to the pressure driven flow for both cases. In the case of flat tip, a local high heat transfer region is observed near the pressure side and the leading edge of the blade tip owing to subsequent reattachment of separated flow related to vertical flow structures. A Similar distribution was also observed by Krishnababu et al. [4].

As it can be seen in Figure 14, high heat transfer region near the pressure side of the squealer rim disappears for the optimum squealer geometry. Even though there is a local high heat transfer region near the leading edge of the squealer rim because of the flow impingement of tip leakage vortex, it is insignificant in comparison to flat tip. Therefore, it can be concluded that the optimum squealer geometry has provided a superior improvement in heat transfer compared to the flat tip geometry.

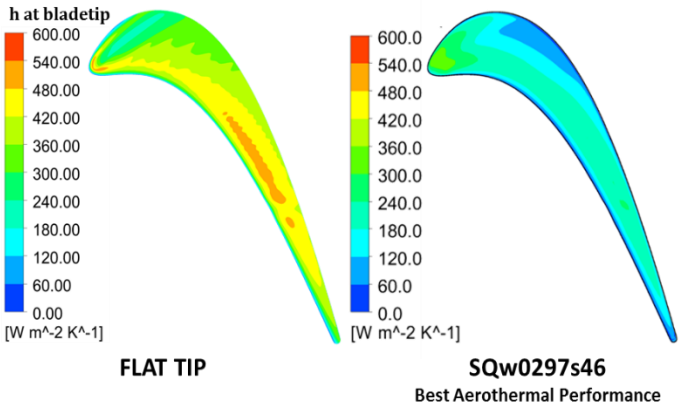

Figure 14. Heat transfer coefficient at blade tip.

CONCLUSION

An artificial intelligence based optimization strategy to identify squealer geometries with optimal aerothermal performances is presented and demonstrated in this paper. An in-house developed multi-objective optimization code based on the NSGA-II algorithm and Artificial Neural Network (ANN) are coupled and used for this purpose. The initial database and the detailed tip clearance flows for the selected geometries was obtained using the commercial

CFD code ANSYS CFX. In order to validate the numerical computations, a well-known test case, Durham cascade, investigated in end wall profiling studies has been used.

Numerical calculations proved that when database is poor, a mean square error calculation only with test data of ANN is not enough for selecting a best network for accurate predictions. Consequently, training data was also added to mean square error calculations and the best ANN was selected according to the weighted average of the mean square error of test and training data. However, the optimum weights for such an average are not sought for in this study.

This study has mainly shown the potential of the squealer geometries in improving the aerothermal performance of blades. The complexity of the blade tip flows showed the importance of artificial intelligence and population based multi-objective optimization strategies for blade tip geometries. However, one must also take into account manufacturability in addition to the heat transfer aspects and turbine aerodynamics to find an appropriate solution to problems generated by tip leakage flow.

In the future studies, fully contoured blade tip shapes will be investigated using 3-D optimization in order to reduce the aerodynamic loss and the thermal loads on the blade tip surface. Also, partial squealer designs with variable positions, thicknesses, and widths will be explored.

ACKNOWLEDGEMENT

This work was funded by TAI DKTM under Grant Number DKTM/2014/05.

NOMENCLATURE

AFTRF	Axial Flow Turbine Research Facility in Turbomachinery Heat Transfer Laboratory in PSU
ANN	artificial neural network
C	blade chord
C_p	pressure coefficient
C_x	blade axial chord
Exit Plane	plane located 0.05Cx downstream of the trailing edge
GA	genetic algorithm
h	local heat transfer coefficient
$\bar{h}$	average heat transfer coefficient
Inlet Plane	located at inlet section of computational domain
MSE	mean square error
MSE_{new}	mean square error calculated from training & test data
NSGA-II	non-dominated sorting genetic algorithm 2
q_w	local wall heat flux
s	squealer rim height
$T_{0,in}$	inlet mass flow averaged total temperature
T_w	wall temperature
w	squealer rim width
ΔC_{p0}	total pressure loss coefficient

REFERENCES

[1] Mischo, B., Behr, T., & Abhari, R. S. (2008). Flow physics and profiling of recessed blade tips: impact on performance and heat load. Journal of Turbomachinery, 130(2), 021008.

[2] Schabowski, Z., & Hodson, H. (2014). The reduction of over tip leakage loss in unshrouded axial turbines using winglets and squealers. Journal of Turbomachinery, 136(4), 041001.

[3] Heyes, F. J. G., Hodson, H. P., & Dailey, G. M. (1991, June). The effect of blade tip geometry on the tip leakage flow in axial turbine cascades. In ASME 1991 International Gas Turbine and Aeroengine Congress and Exposition (pp. V001T01A052-V001T01A052). American Society of Mechanical Engineers.
[4] Krishnababu, S. K., Newton, P. J., Dawes, W. N., Lock, G. D., Hodson, H. P., Hannis, J., & Whitney, C. (2009). Aerothermal investigations of tip leakage flow in axial flow turbines—part I: effect of tip geometry and tip clearance gap. Journal of Turbomachinery, 131(1), 011006.
[5]Azad, G. S., Han, J. C., Bunker, R. S., & Lee, C. P. (2002). Effect of squealer geometry arrangement on a gas turbine blade tip heat transfer. Journal of heat transfer, 124(3), 452-459.
[6] Key, N. L., & Arts, T. (2006). Comparison of turbine tip leakage flow for flat tip and squealer tip geometries at high-speed conditions. Journal of Turbomachinery, 128(2), 213-220.
[7] Denton, J. D. , (1993). Loss mechanisms in turbomachines. ASME Journal of Turbomachinery, 115, 621-656.
[8] Moore, J. O. H. N., & Tilton, J. S. (1988). Tip leakage flow in a linear turbine cascade. Journal of turbomachinery, 110(1), 18-26.
[9] Bindon, J. P. (1989). The measurement and formation of tip clearance loss. Journal of turbomachinery, 111(3), 257-263.
[10] Yaras, M. I.; Sjolander, S. A. (1992). Prediction of tip leakage losses in axial turbines. ASME Journal of Turbomachinery, 114(1), 204-210.
[11] Tallman, J.; Lakshminarayana, B. (2001). Numerical simulation of tip leakage flows in axial flow turbines, with emphasis on flow physics: part 1 – Effect of tip clearance height. ASME Journal of Turbomachinery, 123, 314-323.
[12] Lakshminarayana, B. (1996). Fluid dynamics and heat transfer of turbomachinery; Wiley: New York.
[13] Yaras, M. I., & Sjolander, S. A. (1992). Effects of simulated rotation on tip leakage in a planar cascade of turbine blades: part I—tip gap flow. Journal of Turbomachinery, 114(3), 652-659.
[14] Ameri, A. A., Steinthorsson, E., & Rigby, D. L. (1998). Effect of squealer tip on rotor heat transfer and efficiency. Journal of Turbomachinery, 120(4), 753-759.
[15] Camci, C., Dey, D., & Kavurmacioglu, L. (2005). Aerodynamics of tip leakage flows near partial squealer rims in an axial flow turbine stage. Journal of Turbomachinery, 127(1), 14-24.
[16] Kavurmacioglu, L., Dey, D., & Camci, C. (2007). Aerodynamic character of partial squealer tip arrangements in an axial flow turbine. Part II: Detailed numerical aerodynamic field visualisations via three dimensional viscous flow simulations around a partial squealer tip. Progress in Computational Fluid Dynamics, an International Journal, 7(7), 374-386.
[17] Lee, S. W.; Kim, S. U. (2010). Tip gap height effects on the aerodynamic performance of a cavity squealer tip in turbine cascade in comparison with plane tip results: part I – tip gap flow structure. Experiments in Fluids, 49, 1039-1051.
[18] Zhou, C., & Hodson, H. (2012). Squealer geometry effects on aerothermal performance of tip-leakage flow of cavity tips. Journal of Propulsion and Power, 28(3), 556-567.
[19] De Maesschalck, C., Lavagnoli, S., & Paniagua, G. (2015). Blade tip carving effects on the aerothermal performance of a transonic turbine. Journal of Turbomachinery, 137(2), 021005.
[20] De Maesschalck, C., Lavagnoli, S., Paniagua, G., Verstraete, T., Olive, R., & Picot, P. (2016). Heterogeneous optimization strategies for carved and squealer-like turbine blade tips. Journal of Turbomachinery, 138(12), 121011.
[21] Deb, K., Pratap, A., Agarwal, S., & Meyarivan, T. A. M. T. (2002). A fast and elitist multiobjective genetic algorithm: NSGA-II. IEEE transactions on evolutionary computation, 6(2), 182-197.
[22] Datta, R., & Regis, R. G. (2016). A surrogate-assisted evolution strategy for constrained multi-objective optimization. Expert Systems with Applications, 57, 270-284.
[23] Zhou, A., Qu, B. Y., Li, H., Zhao, S. Z., Suganthan, P. N., & Zhang, Q. (2011). Multiobjective evolutionary algorithms: A survey of the state of the art. Swarm and Evolutionary Computation, 1(1), 32-49.
[24] Lwin, K., Qu, R., & Kendall, G. (2014). A learning-guided multi-objective evolutionary algorithm for constrained portfolio optimization. Applied Soft Computing, 24, 757-772.
[25]nsga-ii--a-multi-objective-optimization-algorithm (Accessed March 2017). http://www.mathworks.com/matlabcentral/fileexchange /10429.

[26] Yan, J. (1999). The effect of end wall profiling on secondary flow in nozzle guide vanes. PhD Thesis, Durham University, England.
[27] Tehlah, N., Kaewpradit, P., & Mujtaba, I. M. (2016). Artificial neural network based modeling and optimization of refined palm oil process. Neurocomputing, 216, 489-501.
[28] Bagheri, M., Mirbagheri, S. A., Bagheri, Z., & Kamarkhani, A. M. (2015). Modeling and optimization of activated sludge bulking for a real wastewater treatment plant using hybrid artificial neural networks-genetic algorithm approach. Process Safety and Environmental Protection, 95, 12-25.
[29] Avcı, H., Kumlutaş, D., Özer, Ö., & Özşen, M. (2016). Optimisation of the design parameters of a domestic refrigerator using CFD and artificial neural networks. International Journal of Refrigeration, 67, 227-238.
[30] Tao, Y., Wang, P., Wang, J., Wu, Y., Han, Y., & Zhou, J. (2017). Combining various wall materials for encapsulation of blueberry anthocyanin extracts: Optimization by artificial neural network and genetic algorithm and a comprehensive analysis of anthocyanin powder properties. Powder Technology, 311, 77-87.
[31] Gossard, D., Lartigue, B., & Thellier, F. (2013). Multi-objective optimization of a building envelope for thermal performance using genetic algorithms and artificial neural network. Energy and Buildings, 67, 253-260.
[32] Asadi, E., da Silva, M. G., Antunes, C. H., Dias, L., & Glicksman, L. (2014). Multi-objective optimization for building retrofit: A model using genetic algorithm and artificial neural network and an application. Energy and Buildings, 81, 444-456.
[33] Magnier, L., & Haghighat, F. (2010). Multiobjective optimization of building design using TRNSYS simulations, genetic algorithm, and Artificial Neural Network. Building and Environment, 45(3), 739-746.